Remote Sensing-Based Estimation of Sorghum LAI Using NDVI from Sentinel-2 and Regression Analysis in GEE

Chandrakant Raj
Tamil Nadu Agricultural University
K Boomiraj
kb78@tnau.ac.in
Tamil Nadu Agricultural University
S Pazhnivelan
Tamil Nadu Agricultural University
Sathyamoorthy N. K
Tamil Nadu Agricultural University
M Prasanthrajan
Tamil Nadu Agricultural University
A Vashisth
ICAR-Indian Agricultural Research Institute
P Krishnan
ICAR-Indian Agricultural Research Institute
J Gayathri
Anna University
G Karthikeyan
Tamil Nadu Agricultural University
S Satheesh
Tamil Nadu Agricultural University

Research Article

Keywords: Leaf Area Index (LAI), NDVI, Sentinel-2, Google Earth Engine, Remote sensing

Posted Date: August 14th, 2025

DOI: https://doi.org/10.21203/rs.3.rs-6756961/v1

Additional Declarations: No competing interests reported.

Version of Record: A version of this preprint was published at Applied Geomatics on May 9th, 2026. See the published version at https://doi.org/10.1007/s12518-026-00730-1.

REMOTE SENSING-BASED ESTIMATION OF SORGHUM LAI USING NDVI FROM SENTINEL-2 AND REGRESSION ANALYSIS IN GEE

Chandrakant Raj H[1], Boomiraj K[2*], Pazhnivelan S[3], Sathyamoorthy N.K[4], Prasanthrajan M[2], Vashisth A [1], Krishnan P [1], Gayathri J[5] Karthikeyan G[2] and Satheesh S[3]

[1]Division of Agricultural Physics, ICAR-Indian Agricultural Research Institute, New Delhi 110012, India. (CRH: chandrakantraj98@gmail.com; AV: ananta.iari@gmail.com; PK: prameelakrishnan@yahoo.com)

[2]Department of Environmental Sciences, Tamil Nadu Agricultural University, Coimbatore 641003, India. (BK: kb78@tnau.ac.in; KG: karthisatbhata@gmail.com; PM: prasanthrajan.m@tnau.ac.in)

[3]Centre for Water and Geospatial Studies, Tamil Nadu Agricultural University, Coimbatore 641003, India. (PS: pazhanivelans@gmail.com; SS: satheeshs2907@gmail.com)

[4]Agro Climate Research Centre, Tamil Nadu Agricultural University, Coimbatore 641003, India. (SNK: nksacrc@gmail.com)

[5] Centre for Climate Change and Disaster Management, Anna University, Chennai 600025,India (GJ: gayathrij26821@gmail.com)

***Corresponding Author:** kb78@tnau.ac.in

Abstract:

The rapid advancement of digital technologies in agriculture has transformed crop monitoring, particularly through the use of remote sensing and Geographic Information Systems (GIS). These tools have proven indispensable in assessing crop growth dynamics, especially in resource-constrained, semi-arid regions. Among climate-resilient crops, sorghum plays a pivotal role in ensuring food and nutritional security under erratic rainfall and limited irrigation conditions. Monitoring its growth using satellite-derived vegetation indices enables real-time, large-scale assessments that are critical for informed decision-making. This study employed the Google Earth Engine (GEE) platform for the retrieval and processing of Sentinel-2 NDVI data to evaluate its effectiveness in estimating Leaf Area Index (LAI), a key biophysical parameter closely linked to crop vigor and productivity. The primary objective was to determine the most appropriate regression model to establish the relationship between NDVI and LAI. A total of 160 field-observed LAI measurements were collected across two districts of Maharashtra, India—Solapur and Ahmednagar—representing varied agro-ecological conditions. Regression analysis revealed that second-order polynomial models outperformed linear, logarithmic, exponential, and power models, with higher R^2 values (> 0.40) and lower RMSE (0.83–0.89) in district-level analysis. The combined dataset showed moderate performance (R^2 > 0.25, RMSE = 1.20), reflecting the influence of spatial variability. NDVI-based crop area classification showed high accuracy, with Kappa coefficients exceeding 0.70, and sorghum areas were estimated at 2,58,925 ha in Solapur and 1,48,475 ha in Ahmednagar, aligning within 5% of official government statistics. These results highlight the value of integrating NDVI and LAI through

polynomial regression models for accurate, real-time crop monitoring, supporting climate-smart agriculture, precision farming, and policy-level planning in semi-arid regions.

Key Words: Leaf Area Index (LAI) ; NDVI; Sentinel-2; Google Earth Engine; Remote sensing

1. Introduction

In the era of rapid digital transformation, technologies like Geographic Information Systems (GIS) and remote sensing are playing a pivotal role in managing environmental and agricultural resources (Klerkx et al., 2019). These tools offer precise, cost-effective, and spatio-temporally rich data, enabling advanced crop monitoring, productivity enhancement, and support for food security (Han et al., 2024; Mehedi et al., 2024). Widely adopted by researchers and policymakers, they help assess crop health, analyze growth dynamics (Na et al., 2024), and mitigate climate change effects (Jiang et al., 2018).

Sorghum stands out as a climate-resilient crop, capable of thriving under drought and saline conditions (Shaw et al., 2024). It is crucial for food and nutritional security in arid and semi-arid regions, particularly for impoverished populations (Gautam & Singh, 2018). Its resilience to diverse climatic and soil conditions has increased its relevance in climate adaptation research (Gautam et al., 2018). Monitoring growth parameters like Leaf Area Index (LAI) is essential for optimizing yield and forecasting production outcomes. Traditionally, LAI is estimated through field-based methods involving sample collection and mathematical calculations (Meiyan et al., 2022), or indirectly using tools like ceptometers (Welles & Norman, 1991). However, these approaches are time-consuming, labor-intensive, and spatially limited. In contrast, remote sensing enables large-scale, efficient LAI estimation through satellite-based platforms (Denis et al., 2020).

Vegetation Indices (VIs) such as the Normalized Difference Vegetation Index (NDVI) are commonly used for estimating LAI, leveraging spectral reflectance characteristics—high absorption in the red band (due to chlorophyll) and high reflectance in the near-infrared (due to leaf mesophyll) (Aklilu Tesfaye & Gessesse Awoke, 2021; Bobée et al., 2012; Delegido et al., 2013). While these indices are widely applied in crops like wheat (Jitendra & Pant, 2024), maize (Mondschein et al., 2024), rice (Boonma et al., 2024), and groundnut (Ekwe et al., 2024), sorghum-specific satellite-based studies remain limited. Nonetheless, LAI integration into crop simulation models (Singh et al., 2024) and machine learning approaches (Brinkhoff et al., 2024) underscores its importance for phenological assessment and yield estimation.

Sentinel-2, launched in 2015 under ESA's Copernicus Programme, provides multispectral imagery at a 290 km swath width (Immitzer et al., 2016; Drusch et al., 2012). In the same year, Google Earth Engine (GEE) emerged as a cloud-based platform for geospatial analysis, featuring a user-friendly JavaScript interface and API access (Gorelick et al., 2017). GEE facilitates efficient processing and visualization of large-scale satellite data and supports diverse applications—crop monitoring, AI-based modeling (ANN, SVM) (Shelestov et al., 2017), LULC classification (Ganjirad & Bagheri, 2024), crop diversification (Jin et al., 2019), soil salinity (Aksoy et al., 2022), lake area estimation (Zhao et al., 2024), and soil erosion studies (Wang & Zhao, 2020). It significantly reduces the computational load in big-data geospatial analysis (Awad, 2021).Though LAI estimation has typically relied on linear regression models using NDVI or EVI (Bajocco et al., 2022; Alexandridis et al., 2020), these relationships are often non-linear due to variability in crops, phenology, and management practices. Hence, flexible modeling is needed. This study therefore aims to: (i) Estimate crop acreage using NDVI in a semi-arid region; (ii)Evaluate the NDVI–LAI relationship using multiple regression approaches.

2. Materials and Method

2.1. Study Area

The study was conducted in Ahmednagar and Solapur districts (Fig. 1) in Maharashtra, key producers of Rabi sorghum, contributing nearly 50% of India's seasonal output. Located between 17.65°–19.10° N and 74.74°–75.90° E, these districts exhibit distinct agro-climatic and edaphic characteristics. Solapur is dominated by medium-deep, potash-rich but nitrogen-deficient murrum soils, covering about 46% of the region. Ahmednagar has diverse soils—from shallow red and grey to deep black—and relatively better irrigation in the north, supporting crops like wheat and sugarcane. However, field verification confirmed that sorghum predominates in the south, where irrigation is limited.Annual rainfall ranges from 600–700 mm, typical of semi-arid zones, making the region suitable for grain-pulse or pulse-grain systems, which are more sustainable under limited water availability—conditions ideal for drought-tolerant Rabi sorghum cultivation.

2.2 Data Collection and Analysis

2.2.1 Ground Verified data

Ground truthing was conducted through two field surveys across district road networks, focusing on village-level crop data, primarily sorghum. Leaf Area Index (LAI) was measured using a standardized protocol by recording the length and width of the fully expanded apical leaflet of the third tetrafoliate leaf. Specifically, the length and width of the fully expanded apical leaflet of the third tetrafoliate leaf were measured, following the established protocol detailed below.

$$\mathrm{LAI} = 0.7 \times \frac{\mathrm{L \times W \times B \times n}}{\mathrm{Spacing\ (cm)}} \qquad \text{----------} \qquad (1)$$

where,

L - Length of the leaf (cm),

W -Width of the leaf (cm),

n - No. of leaves, Spacing – Plant-Plant/Row-Row (cm)

At least five samples were taken per field during each visit. Spatial LAI values and corresponding GPS coordinates were recorded (Fig. 2). In Solapur, surveys focused mainly on sorghum and barren lands for classification validation. In Ahmednagar, data were collected on multiple crops, including wheat, sugarcane, and onion, reflecting its agricultural diversity. To assess classification accuracy between crop and non-crop areas, a confusion matrix was constructed, presented in the results section. A table summarizing ground-truth data points with corresponding collection dates is also included for reference and validation.

2.3 Satellite Imagery

Sentinel-2, with its open-access policy, offers a cost-effective solution for researchers, particularly when combined with other freely available geospatial datasets (Turner et al., 2015). This study utilized Sentinel-2A imagery to monitor the Rabi cropping season (2022–2023). The spectral bands used in the analysis are detailed in Table 1.

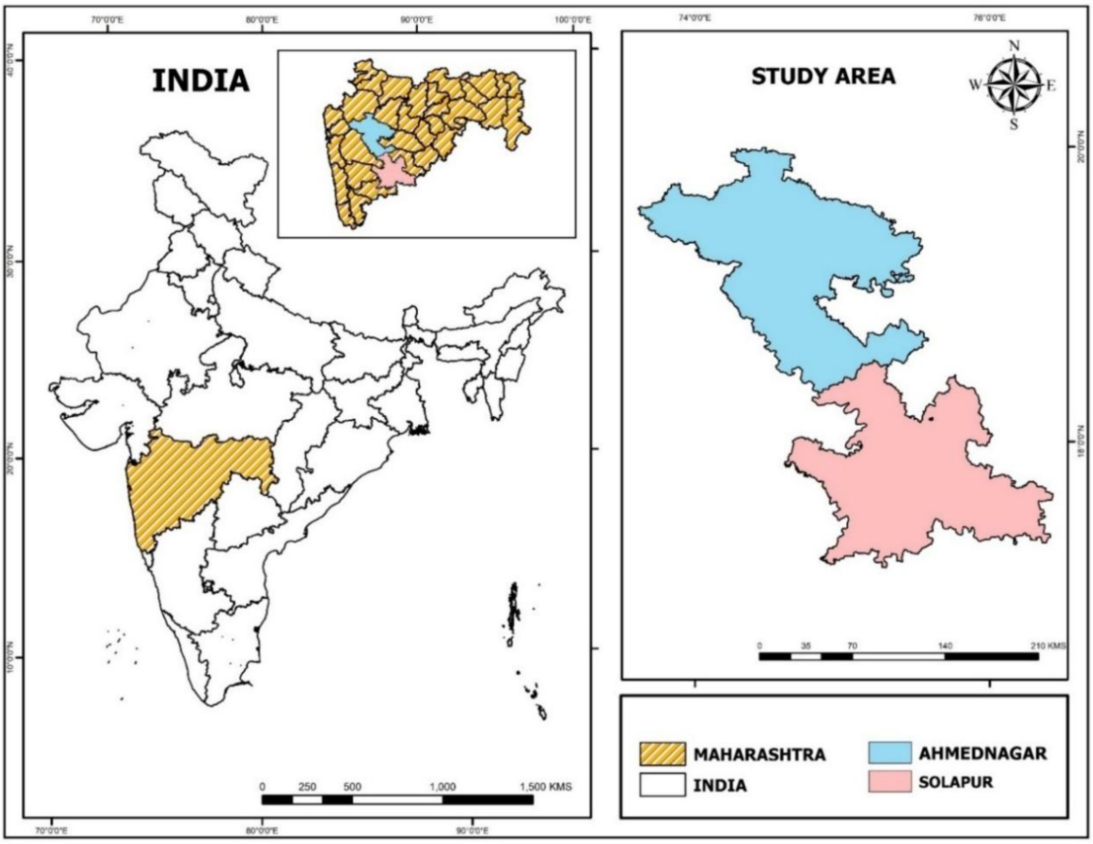

Fig. 1 Depiction of the selected study regions (Ahmednagar and Solapur) in Maharashtra, India

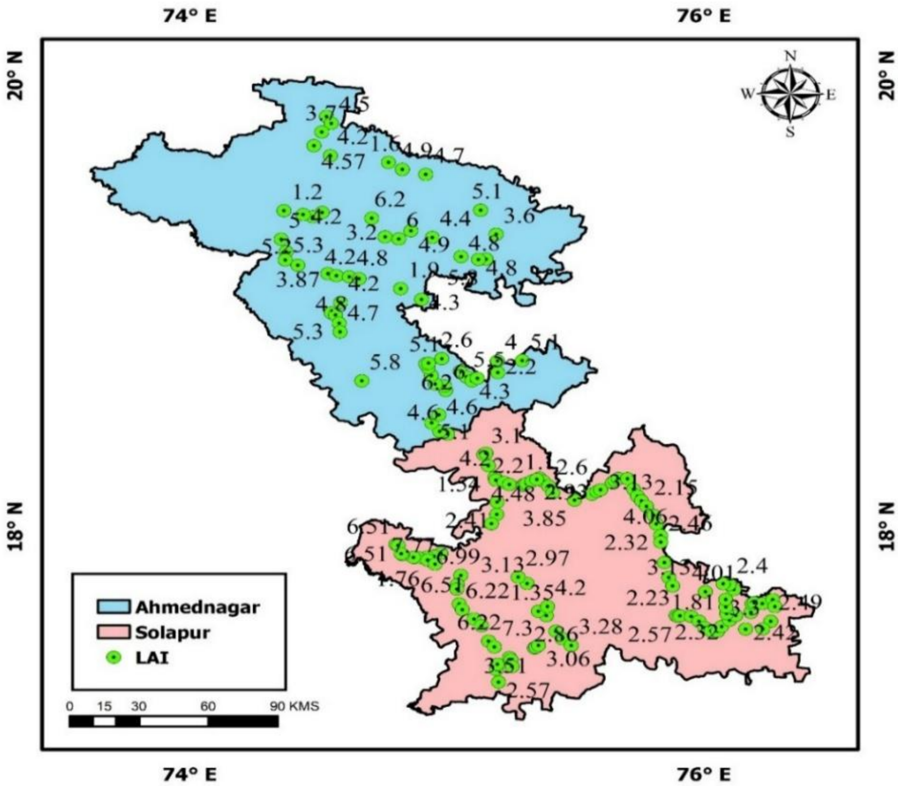

Fig 2. Collection of Ground Truth LAI of sorghum crop at different coordinates in the study regions.

Table 1 Different Bands of sentinel -2A

Sentinel-2A		
Spatial Resolution(m)	**Bands**	**Central wavelength (nm)**
10	Band 2 - Blue	492.4
	Band 3 - Green	559.8
	Band 4—Red	664.6
	Band 8—NIR	832.8
20	Band 6—Red edge	740.5
	Band 7—Red edge	782.8
	Band 8A—Narrow NIR	864.7
	Band 11—SWIR	1613.7
	Band 12—SWIR	2202.4
60	Band 1—Coastal aerosol	442.7
	Band 9—Water vapour	945.1
	Band 10—SWIR—Cirrus	1373.5

2.4 Google earth engine (GEE)

The crop mask delineation process, outlined in Figure 3, began with ground-verified reference points from both districts. While the focus was on Rabi sorghum, additional data on maize, wheat, sugarcane, and barren land were collected over multiple dates to capture crop variability. These georeferenced points supported the Leaf Area Index (LAI) estimation workflow. To ensure spatial precision, all GPS points—originally recorded using a Garmin eTrex device (accuracy ~10 m)—were cross-validated using Google Earth Pro, enhancing the reliability of the dataset for analysis within GEE.

2.4.1. Pre-processing the satellite imagery data in GEE

1. Least Cloud Cover

Pre-processing began with selecting Sentinel-2 Level-2A imagery featuring minimal cloud cover. These surface reflectance products were filtered using the QA60 cloud mask band, excluding pixels with more than 10% cloud cover to ensure high-quality, cloud-free data for analysis. Table 1 outlines the spectral bands used, while Table 2 summarizes satellite acquisition windows, highlighting periods with the least cloud interference over the study area.

Table. 2. Date of Satellite pass on location for which the least cloud cover data was selected

Period	Start Date	End Date
Collection 1	2022-09-16	2022-10-30
Collection 2	2022-10-01	2022-10-15
Collection 3	2022-10-16	2022-10-31
Collection 4	2022-11-01	2022-11-15
Collection 5	2022-11-16	2022-11-30
Collection 6	2022-12-01	2022-12-15
Collection 7	2022-12-16	2022-12-31
Collection 8	2023-01-01	2023-01-15
Collection 9	2023-01-16	2023-01-31
Collection 10	2023-02-01	2023-02-15
Collection 11	2023-03-01	2023-03-15
Collection 12	2023-03-16	2023-03-31

2. Geo referencing: To ensure accurate spatial alignment, all input datasets—including shapefiles and ancillary data—were pre-processed and uploaded using the WGS 84 coordinate system. This spatial referencing ensured full compatibility with the Google Earth Engine (GEE) platform and provided precise geospatial representation for subsequent analyses.

3. Imagery Stacking: Satellite imagery was composited into 15-day intervals to effectively capture the key phenological stages of crop growth. This temporal segmentation allowed for a more detailed representation of the crop development period, facilitating pixel-level analysis of the growing season duration and enabling improved monitoring of growth dynamics.

5. Supervised Classification Using Random Forest: A supervised classification was performed using the Random Forest algorithm (ee.Classifier.smileRandomForest) within Google Earth Engine (GEE). This ensemble-based method, known for its robustness and accuracy in land use/land cover (LULC) classification, functions effectively with minimal machine learning expertise (Gislason et al., 2006; Ahmed et al., 2024; Cui et al., 2023). The resulting crop mask allowed for precise crop area delineation. Rigorous pre-processing and classification steps ensured reliable outputs for crop acreage estimation and land cover mapping.

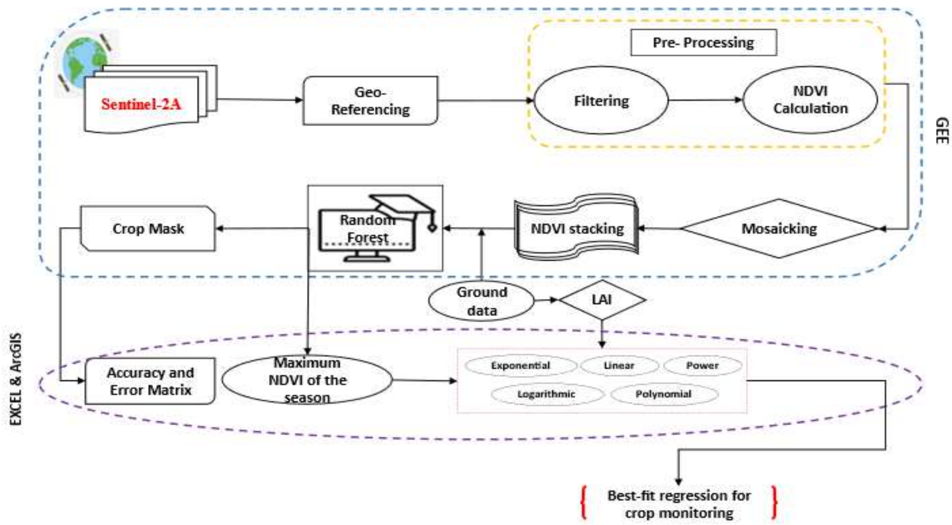

Fig. 3 Flow Chart of the methodology for area and establishing relationships between NDVI and LAI

6. Generation of NDVI: The Normalized Difference Vegetation Index (NDVI) was generated to support the estimation of crop health and growth stages. Based on ground truthing observations, the maximum Leaf Area Index (LAI) for the season was anticipated to occur during Collection 8, corresponding to the first fortnight of January. This period was identified as the peak growth stage for the Rabi sorghum crop, making it optimal for NDVI-based analysis and subsequent correlation with LAI values.

2.5. Accuracy assessment

Classification accuracy was evaluated following the method by Lillesand et al. (2015), using overall accuracy and the Kappa coefficient to assess dataset reliability. Each classified pixel was compared with its corresponding reference class from ground truth data, with 40% of reference points set aside for validation.

An error matrix (confusion matrix) was constructed to measure agreement and disagreement between classification results and ground truth at the pixel level.

From this matrix, the following accuracy metrics were computed:

$$\text{Overall Accuracy (OA):Overall accuracy} = \frac{\Sigma\,(\text{Correctly classified classes along diagonal})}{\Sigma\,(\text{Row Total or Column Total})}$$

This metric reflects the proportion of all correctly classified samples relative to the total number of reference pixels.

Producer Accuracy (PA):

Indicates how well real-world features of a given class are correctly classified.

User Accuracy (UA):

User Accuracy (UA) indicates the likelihood that a pixel classified into a specific class truly represents that class on the ground. Alongside overall accuracy, the Kappa Coefficient (K) was calculated to evaluate how much the classifier outperforms random assignment (Richards & Ferrell, 1999).If there are r rows and the same number of columns in an error matrix.

$$K = \frac{NA - B}{N^2 - B}$$

Where:

A = Sum of diagonal elements (used in overall accuracy)

B = Sum of the products of row and column totals for each class

N = Total number of pixels in the error matrix

This metric provides a robust measure of classification agreement beyond chance.

2.6. Establishment of relationships between the leaf area index (LAI) and Normalized Difference Vegetation Index (NDVI)

Remote sensing is vital for crop monitoring and productivity assessment, with Leaf Area Index (LAI) recognized as a key biophysical parameter (Bajocco et al., 2024; Getahun et al., 2024). NDVI, derived from Sentinel-2's red (Band 4) and NIR (Band 8) reflectance, serves as a widely used indicator of vegetation vigor, while LAI provides a direct physiological measure of canopy structure and photosynthetic potential (Wu et al., 2023). Together, they are essential for understanding vegetation dynamics and modeling crop growth. In this study, 160 ground-based LAI measurements were temporally matched with NDVI values from the same acquisition dates to ensure consistency. The analysis tested the null hypothesis that no significant relationship exists between LAI and NDVI. To explore the nature of this relationship, five regression models were applied; (i)Linear Regression – Assumes a direct proportional link; (ii)Logarithmic Regression – Addresses NDVI saturation at high values; (iii) Exponential Regression – Captures rapid changes at low NDVI; (iv) Power Regression –

Models non-linear canopy development;(v) Polynomial Regression – Represents complex, multi-phase growth patterns.Models were evaluated based on goodness-of-fit metrics to identify the most accurate and biologically meaningful LAI–NDVI relationship.

2.7. Evaluation metrics

Regression model performance was evaluated using standard metrics: coefficient of determination (R^2), Root Mean Square Error (RMSE), and p-values to assess statistical significance. Analyses were conducted separately for Solapur and Ahmednagar, as well as on the combined dataset, allowing insights under varying agro-ecological conditions. Model selection was based on a 95% confidence level ($p < 0.05$). The best-fit model was identified by its high R^2, low RMSE, and statistically significant LAI–NDVI relationship, reflecting both predictive accuracy and biological relevance.

2.7.1. Co-efficient of determination (R^2)

Among evaluation metrics, R^2 is widely used to measure the strength of the relationship between LAI and NDVI. It ranges from 0 to 1, with values closer to 1 indicating a stronger correlation and better model fit. In environmental and agronomic modeling, an R^2 above 0.5 is generally considered acceptable.

$$R^2 = \left(\frac{\sum_{i=1}^{n}(y_i - \bar{y}_i)(\hat{y}_i - \bar{\hat{y}}_i)}{\sigma_{y_i}\sigma_{\hat{y}}} \right)^2$$

y_i = denotes the observed value, $\hat{y}_i$ = predicted value for i = 1, 2, …. n., $\hat{y}_i$and$\overline{\hat{y}_i}$ is the mean of observed and predicted values, $\sigma_{y_i} and\ \sigma_{\hat{y}}$ is the standard deviation of actual and predicted values, respectively.

2.7.2. Root Mean Square Error (RMSE)

RMSE is a key metric for assessing predictive model performance, especially in environmental and agricultural contexts. It measures the average deviation between observed and predicted values, with lower RMSE indicating higher accuracy. By aggregating prediction errors across all data points, RMSE provides a direct and reliable estimate of overall model accuracy. The RMSE is calculated using the following equation:

$$RMSE = \sqrt{\frac{\sum_{i=1}^{n}(y_i - \hat{y}_i)^2}{n}}$$

Here, y_i is the observed value while $\hat{y}_i$ is the predicted value and n shows the number of observations. The unit of RMSE is similar to the unit of observed or predicted values.

3. Results

3.1. Sorghum Area

During the 2022–23 Rabi season, sorghum cultivation was assessed using Sentinel-2A imagery across Solapur and Ahmednagar districts in southern Maharashtra. The estimated area under sorghum was approximately 258,925 hectares in Solapur and 148,475 hectares in Ahmednagar. These estimates were derived through supervised classification using ground-verified crop and non-crop reference points, as shown in Figures 4(b) and 5(b). Solapur recorded the larger sorghum area, accounting for about 52.3% of its total agricultural land. In contrast, Ahmednagar exhibited a notable decline in sorghum cultivation, with the current season showing a reduction of nearly 39.6% compared to previous years when sorghum covered more than half of the agricultural area. Field observations suggest that this decline may be attributed to cropping shifts in the better-irrigated mid, northern, and northwestern regions of Ahmednagar, where farmers have increasingly adopted wheat and sugarcane cultivation. Solapur, on the other hand, relies primarily on residual soil moisture, with only limited irrigated zones, thereby continuing to support substantial Rabi sorghum coverage.

To evaluate the reliability of the classification, a confusion matrix was constructed using 102 validation points in Solapur and 64 in Ahmednagar. The classification accuracy reached 91.1% in Solapur and 84.2% in Ahmednagar, indicating strong agreement with the ground-truth data. The Kappa coefficient, which accounts for agreement beyond chance, was 0.82 for Solapur and 0.74 for Ahmednagar. These results validate the accuracy and robustness of using Sentinel-2 imagery in conjunction with ground-verified reference data for mapping sorghum cultivation, as summarized in Table 3.

3.2. Correlational Analysis

3.2.1. Different regression relationships between the leaf area index (LAI) and normalized difference vegetation Index (NDVI)

This section investigates the relationship between Leaf Area Index (LAI) and Normalized Difference Vegetation Index (NDVI) to enhance sorghum LAI estimation via remote sensing. Regression models were applied to establish functional associations between these variables, supporting improved biophysical assessments. The analysis accounted for contrasting agricultural contexts in Ahmednagar, with better irrigation, and Solapur, dominated by rainfed systems. These agro-ecological differences influence canopy development and spectral reflectance, potentially affecting LAI–NDVI dynamics. To address this variability, models were tested separately for each district and then on a combined dataset to evaluate robustness across diverse environments. Model performance was measured using the coefficient of determination (R^2), assessed at $p < 0.05$ for statistical significance, and Root Mean Square Error (RMSE) to quantify prediction error. This approach aimed to identify regression models adaptable to varying soil and climatic conditions, thereby improving the accuracy and consistency of LAI estimation.

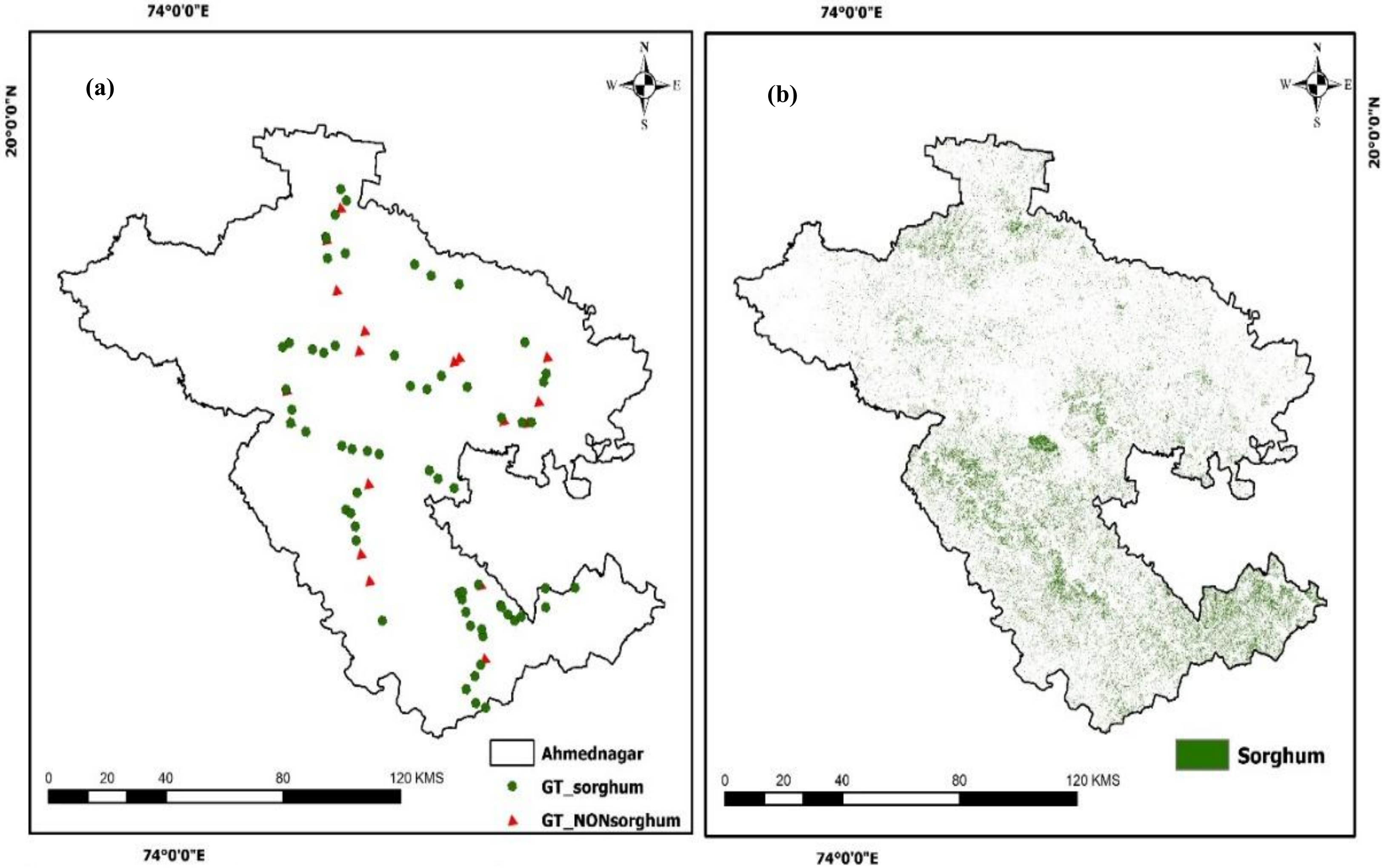

Fig.4 (a) Depiction of Map with ground truth points (Sorghum & Non sorghum) and **(b)** crop mask (*Rabi* - sorghum) at Ahmednagar, Maharashtra, India.

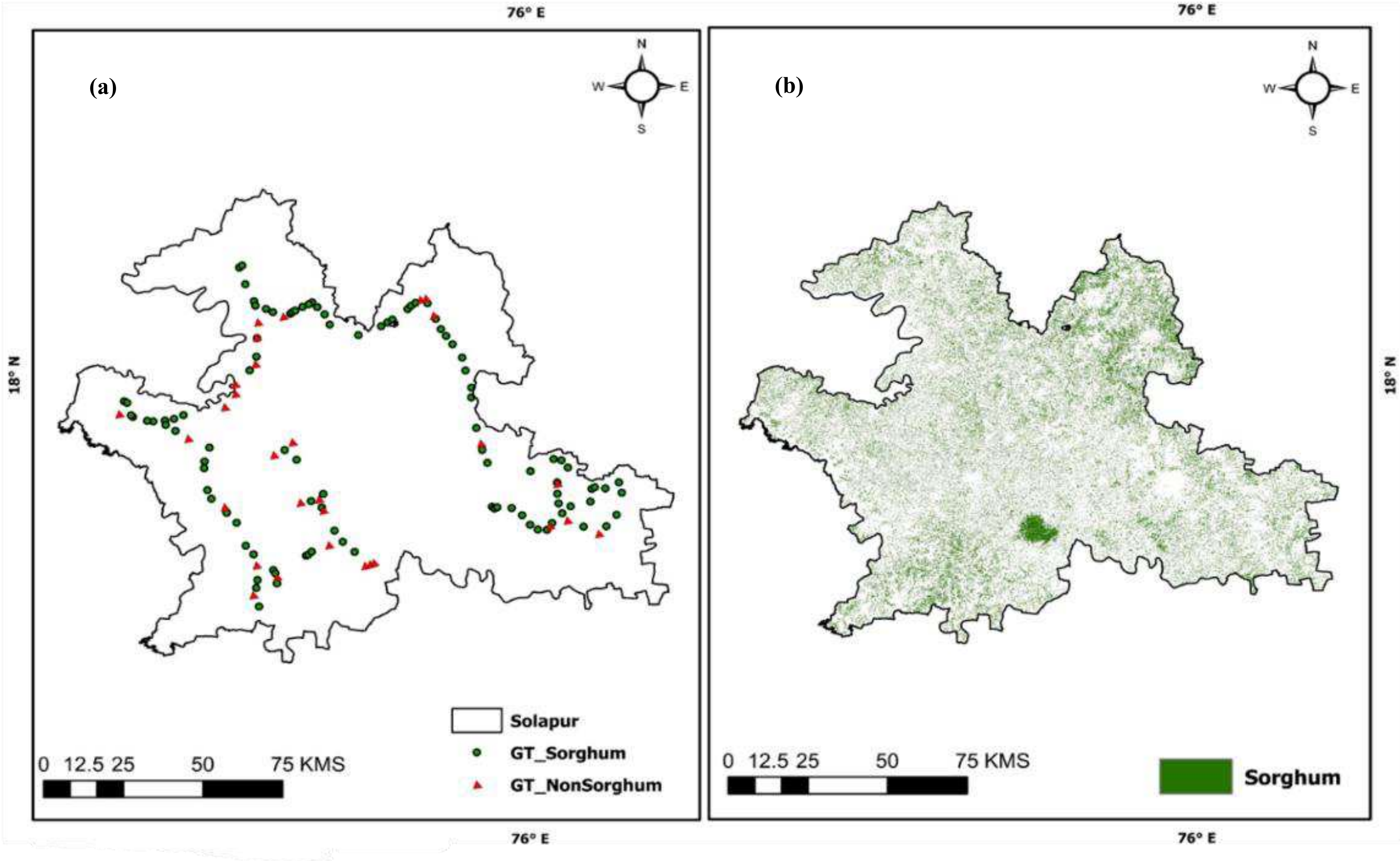

Fig.5 (a) Depiction of Map with ground truth points (Sorghum & Non sorghum) and **(b)** crop mask (*Rabi* - sorghum) at Solapur, Maharashtra, India.

Table 3 Different districts confusion matrix and accuracy

<table>
<tr><th colspan="5">Ahmednagar</th><th colspan="5">Solapur</th></tr>
<tr><td rowspan="5">Actual class from survey</td><td rowspan="2">Crop</td><td colspan="3">Predicted class from the map</td><td rowspan="5">Actual class from survey</td><td rowspan="2">Crop</td><td colspan="3">Predicted class from the map</td></tr>
<tr><td>Sorghum</td><td>Non-Sorghum</td><td>Accuracy</td><td>Sorghum</td><td>Non-Sorghum</td><td>Accuracy</td></tr>
<tr><td>Sorghum</td><td>64</td><td>12</td><td>84.2%</td><td>Sorghum</td><td>102</td><td>15</td><td>87.2%</td></tr>
<tr><td>Non-sorghum</td><td>2</td><td>30</td><td>93.8%</td><td>Non-sorghum</td><td>2</td><td>25</td><td>92.6%</td></tr>
<tr><td>Reliability</td><td>97.0%</td><td>71.4%</td><td>87.0%</td><td>Reliability</td><td>98.1%</td><td>62.5%</td><td>88.2%</td></tr>
<tr><td colspan="3">Average accuracy</td><td colspan="2">89.0%</td><td colspan="3">Average accuracy</td><td colspan="2">89.9%</td></tr>
<tr><td colspan="3">Average reliability</td><td colspan="2">84.2%</td><td colspan="3">Average reliability</td><td colspan="2">80.3%</td></tr>
<tr><td colspan="3">Overall accuracy</td><td colspan="2">87.0%</td><td colspan="3">Overall accuracy</td><td colspan="2">88.2%</td></tr>
<tr><td colspan="3">Kappa index</td><td colspan="2">0.74</td><td colspan="3">Kappa index</td><td colspan="2">0.76</td></tr>
</table>

3.2.2. Ahmednagar region

In Ahmednagar district, field observations showed that the northern irrigated areas had reduced sorghum cultivation, as the crop typically requires less water. However, ground-truth data from these zones indicated high LAI values ranging from 4.5 to 6.2, reflecting robust canopy growth. Despite its limited spatial extent, sorghum's spectral signature in irrigated fields proved effective for assessing vegetation health, structure, and growth stage. To model the LAI–NDVI relationship, four regression approaches—Linear, Logarithmic, Power, and 2nd-order Polynomial—were evaluated. Among these, the polynomial model showed the best performance, with an RMSE of 0.89, indicating strong predictive accuracy (Figure 6d). This model was used to generate a spatial LAI map, illustrating the canopy cover distribution across irrigated and rainfed zones within the district (Figure 8a), offering valuable insight into sorghum's biophysical status.

3.2.3. Solapur region:

In Solapur district, LAI values ranged from 1.1 to 7.7, reflecting a broad variation in crop vigor across both irrigated pockets and largely rainfed areas. This variability highlights the moisture-limited conditions under which sorghum is commonly cultivated in the region. To relate ground-based LAI with Sentinel-2 DN values, four regression models—Linear, Logarithmic, Power, and 2nd-order Polynomial—were tested. The polynomial model again outperformed the others, effectively capturing the non-linear relationship between NDVI and LAI under varying canopy and moisture conditions. As illustrated in Figure 7(d), the model yielded an average RMSE of 0.83, indicating strong alignment between predicted and observed LAI values. Based on this model, a spatial LAI map for Solapur was developed (Figure 8b), offering detailed insights into crop canopy conditions across the district.

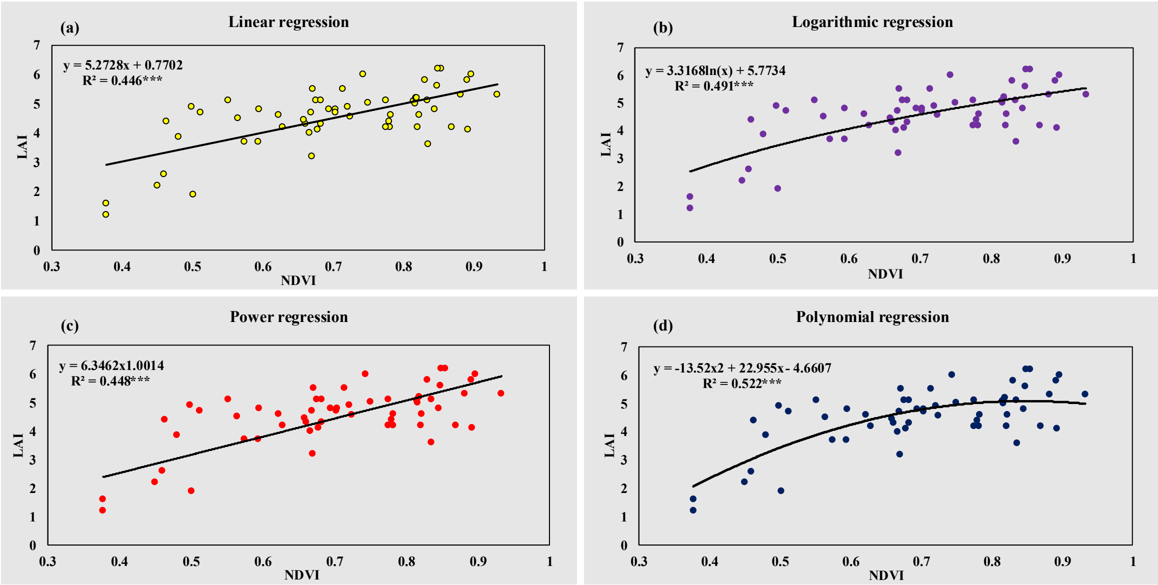

Fig.6 Quantification of LAI from Sentinel-2A derived NDVI for sorghum at peak vegetative stage using different regression approaches (a) Linear, (b) Logarithmic, (c) Power and (d) Polynomial for Ahmednagar, Maharashtra, India

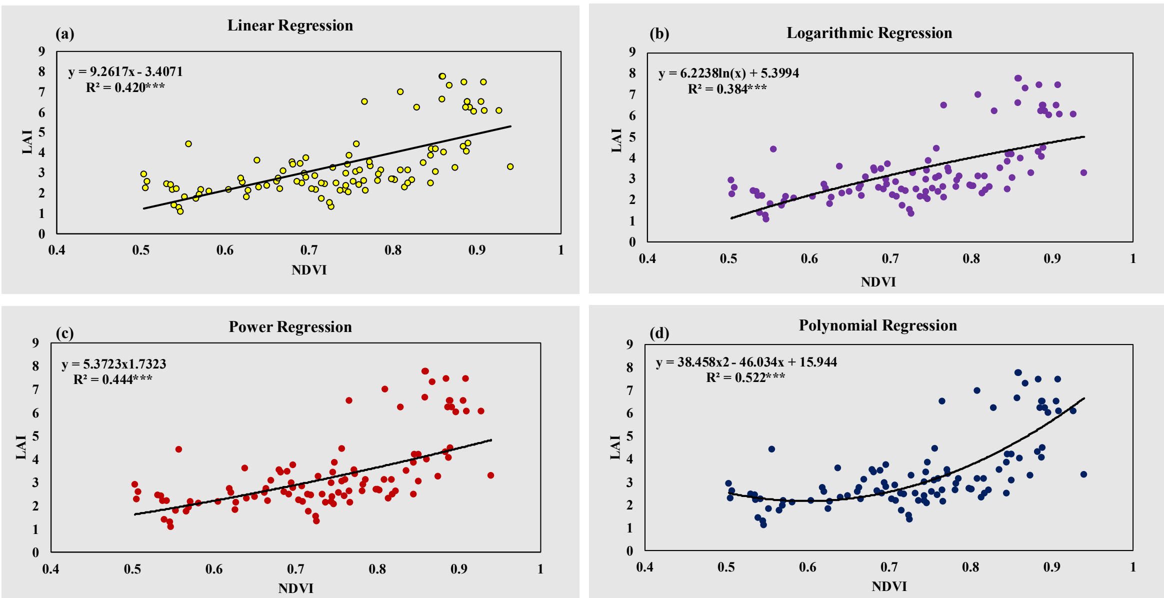

Fig.7 Quantification of LAI from Sentinel-2A derived NDVI for sorghum at peak vegetative stage using different regression approaches (a) Linear, (b) Logarithmic, (c) Power and (d) Polynomial for Solapur, Maharashtra, India.

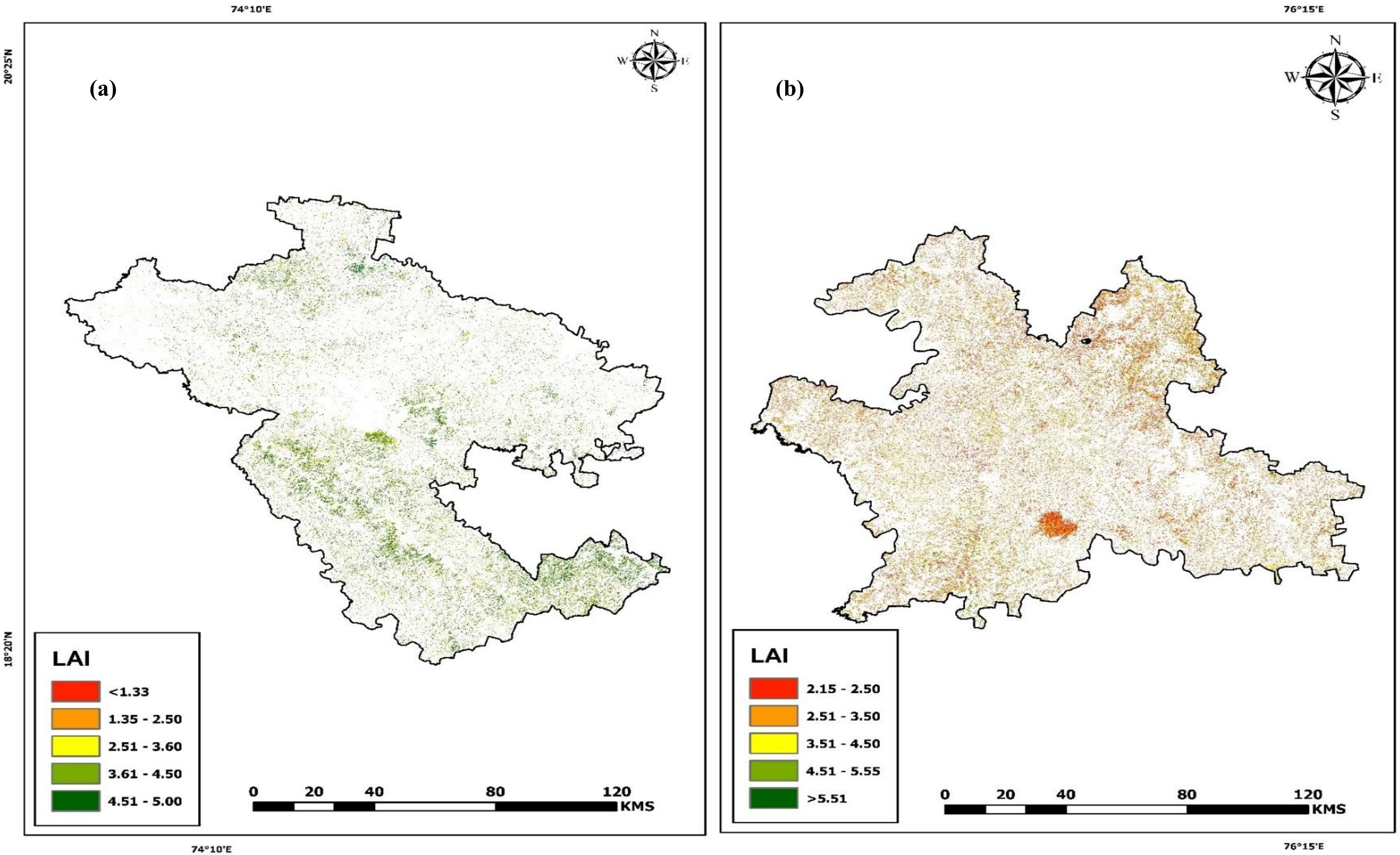

Fig.8 Depiction of LAI generated sample points from distinguished districts (a) Solapur & (b) Ahmednagar, Maharashtra, India individually with common regression approach. Legends showing the LAI matrix for individual district.

3.2.4. Combined results

To evaluate the robustness of the regression models under diversified agro-climatic conditions, satellite imagery acquired on the same Sentinel-2A pass date was used for both Ahmednagar and Solapur. The datasets underwent identical statistical analyses to determine whether the regression models maintained performance consistency across contrasting environments. Among the tested models, the polynomial regression (2nd order) again yielded the best performance, with a coefficient of determination (R^2) > 0.32 at a statistical significance level of $p < 0.05$, as illustrated in Figure 9(d). Although the R^2 value was lower than the district-level models—likely due to increased heterogeneity—the model still provided a reasonable fit across the combined dataset. The average RMSE for predicted LAI in the combined analysis was 1.20, indicating moderate predictive error when generalizing across regions. Using the polynomial regression equation derived from the merged dataset, a combined spatial LAI map was generated. This map integrated both Ahmednagar and Solapur, with distinct legends for each district, enabling comparative visual interpretation of canopy structure and crop vigor. The final combined spatial output is presented in Figure 10.

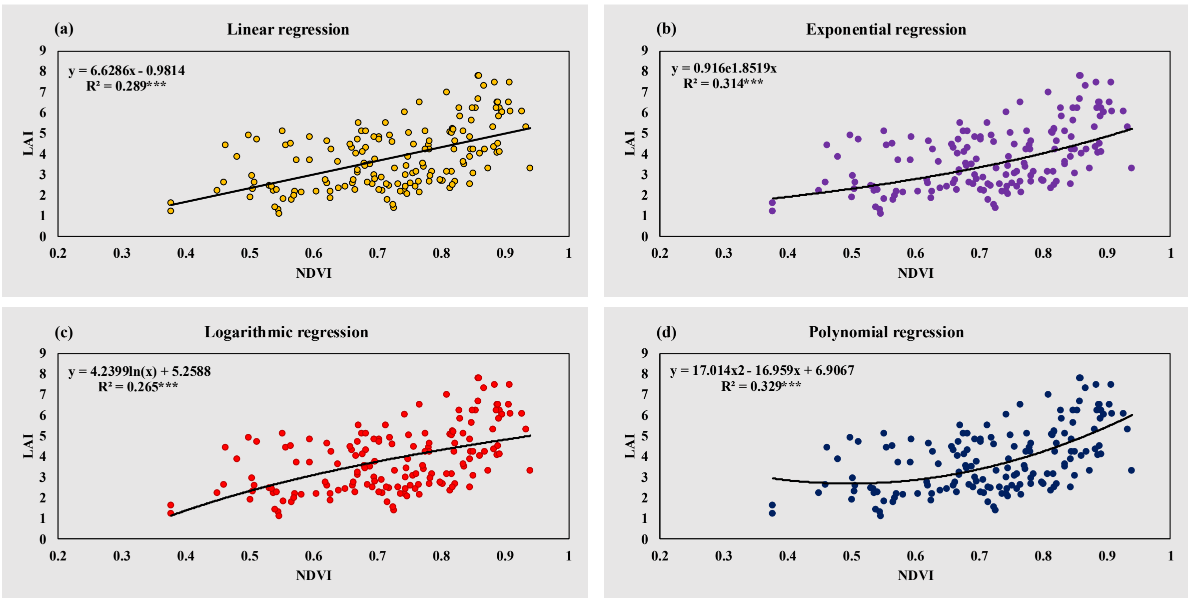

Fig.9 Quantification of LAI from Sentinel-2A derived NDVI for sorghum at peak vegetative stage using different regression approaches (a) Linear, (b) Logarithmic, (c) Power and (d) Polynomial for both districts Ahmednagar & Solapur, Maharashtra, India.

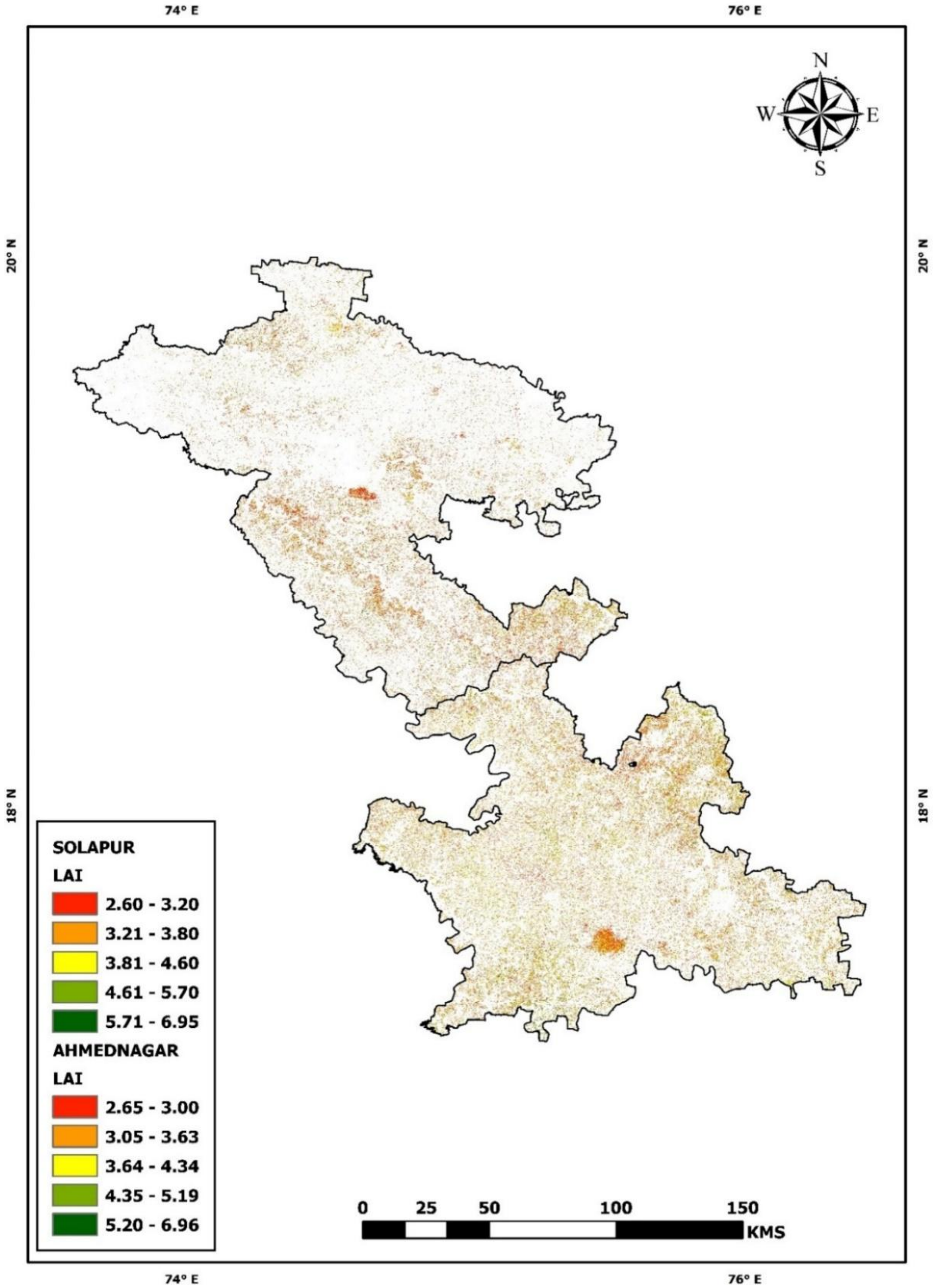

Fig.10 Depiction of LAI generated from combined LAI points of this districts (Solapur & Ahmednagar, Maharashtra, India) with with Google Earth Engine (GEE) to estimate the area of sorghum crops and quantify the Leaf Area Index (LAI).

4. Discussion

This study provides valuable insights into the interaction between the Normalized Difference Vegetation Index (NDVI) and Leaf Area Index (LAI) for Rabi sorghum in the semi-arid regions of

Maharashtra, leveraging Sentinel-2A imagery and the cloud-based Google Earth Engine (GEE) platform. The methodology demonstrates that combining freely available satellite data with ground-truth measurements and cloud computing tools can enable scalable, timely, and cost-effective crop monitoring systems applicable in data-scarce and resource-limited contexts. The use of GEE allowed for efficient data handling, storage, and processing, overcoming traditional limitations associated with downloading and managing high-resolution satellite datasets. Its integration with Sentinel-2 Level-2A surface reflectance imagery, which includes 10–20 m resolution bands relevant for vegetation analysis, ensured detailed, frequent, and accurate monitoring of canopy development throughout the 2022–23 Rabi season. This aligns with the growing body of literature emphasizing cloud-based remote sensing platforms for large-scale agricultural applications (Maciel Junior et al., 2024; Wang et al., 2024). By utilizing Sentinel-2 data, this study covered heterogeneous cropping systems over large areas, providing a synoptic view of spatio-temporal vegetation dynamics at district and inter-district scales. Leaf Area Index (LAI) serves as a critical indicator of crop productivity, photosynthetic potential, and transpiration. It is a direct measure of the canopy structure and, when coupled with vegetation indices, facilitates non-destructive, spatially continuous estimation of crop health.

LAI has long been integrated into crop growth simulation models, yield forecasting systems, and resource use efficiency studies. For example, it serves as a key input in productivity efficiency models (PEM) (Dong et al., 2016), data assimilation frameworks and Crop Cutting Experiments (CCE) aimed at enhancing national yield estimation programs (Pazhanivelan et al., 2025). The strong correlation found in this study between NDVI and LAI ($p < 0.01$) supports the utility of NDVI as a proxy variable in such modeling applications, particularly in regions with limited access to continuous field measurements. High classification accuracy (>85%) and Kappa coefficients (>0.70) reflect the robustness of the GEE-based supervised classification approach. The use of Random Forest (RF) classifiers, trained on 160 field-collected points, resulted in high-precision crop mask generation across both Solapur and Ahmednagar. These findings are in line with previous studies that have employed RF in combination with NDVI and ground-truth data to classify cropland and estimate yields (Maciel Junior et al., 2024).

The spatial heterogeneity observed—particularly the lower sorghum coverage in irrigated areas of Ahmednagar versus the moisture-dependent cultivation in Solapur—highlights the need for region-specific calibration of models to reflect agro-ecological diversity. Ground surveys conducted during peak phenological stages ensured that NDVI and LAI were synchronized temporally, enhancing model accuracy. Among the tested regression models, the second-order polynomial regression consistently outperformed linear and non-linear alternatives in all scenarios, capturing the non-linear nature of NDVI-LAI relationships. This behavior is well-documented, particularly in crops with high LAI saturation, where NDVI tends to flatten beyond certain canopy densities. The district-level models showed lower RMSE and higher R^2 values (Ahmednagar RMSE = 0.89; Solapur RMSE =

0.83) compared to the combined model (RMSE = 1.20, $R^2 > 0.32$), reflecting greater consistency within homogeneous regions. However, the combined model still performed adequately, offering a generalized relationship applicable at the district-cluster or regional scale.

NDVI remains one of the most commonly used vegetation indices due to its simplicity and sensitivity to chlorophyll content. In this study, NDVI values below 0.3 were generally associated with non-photosynthetic surfaces—consistent with findings from Jones et al. (2024). The robustness of the NDVI–LAI relationship in this work adds to a growing body of evidence supporting NDVI as a cost-effective, scalable proxy for canopy characterization in sorghum and similar crops. Nevertheless, NDVI has known saturation effects at high LAI values, and its performance may vary across crop types, growth stages, and soil backgrounds (Tenreiro et al., 2021). Other indices like NDRE, NRI, or GRVI offer improved sensitivity under specific conditions, and their integration—possibly through multi-index fusion or machine learning approaches—represents a key future research direction. Future studies should explore the use of alternative vegetation indices, higher-resolution datasets (e.g., PlanetScope, Sentinel-1 SAR, Landsat-9), and machine learning models such as Support Vector Machines, XGBoost, or deep learning frameworks. The inclusion of ancillary data such as soil moisture, temperature, and crop management records could improve predictive performance and enable multivariate modeling. Additionally, the application of recursive feature elimination (RFE) and other feature selection algorithms can optimize input selection for LAI estimation (Khan et al., 2024). The development of automated workflows in GEE for continuous crop monitoring could also assist policymakers in resource allocation, insurance modeling, and climate adaptation strategies. In the long term, integrating such approaches with national-level yield forecasting systems would strengthen climate-smart agriculture initiatives, ensuring food security and sustainable resource use in climate-vulnerable regions like semi-arid Maharashtra.

5. Conclusion:

This study demonstrated the effectiveness of integrating Sentinel-2 MSI data and NDVI for estimating Leaf Area Index (LAI) and monitoring sorghum growth in the semi-arid districts of Solapur and Ahmednagar, Maharashtra. Utilizing the capabilities of Google Earth Engine (GEE), large-scale satellite data were processed efficiently to derive timely, biophysical crop parameters. Among the regression models evaluated, the second-order polynomial regression consistently outperformed others, accurately capturing the non-linear NDVI–LAI relationship. District-level models yielded the highest performance, with $R^2 > 0.40$ and RMSE values between 0.83 and 0.89, while the combined model showed acceptable performance ($R^2 > 0.32$, RMSE = 1.20), indicating the impact of localized agroecological factors like irrigation, soil variability, and management practices.

Supervised classification in GEE enabled precise crop area delineation, estimating 258,925 ha of sorghum in Solapur and 148,475 ha in Ahmednagar. These estimates closely aligned with government records, showing less than 5% deviation and Kappa coefficients above 0.70, confirming the reliability of the approach. The results highlight GEE's effectiveness as a scalable and accessible platform for agricultural monitoring in data-scarce, semi-arid regions, eliminating challenges related to data acquisition and pre-processing. The robust NDVI–LAI model established here improves sorghum monitoring accuracy and supports adaptive management under climate variability. The findings offer significant potential for yield prediction, crop insurance modeling, and resource optimization, informing policy decisions such as adjusting Minimum Support Price (MSP) or targeting inputs efficiently. Future work should explore additional vegetation indices like NDRE, GRVI, and EVI for better sensitivity across crop stages. Integration of machine learning, recursive feature elimination, and data assimilation with crop models could further refine LAI prediction. Expanding this framework to other crops and regions will enhance its applicability, supporting digital agriculture, food security, and sustainable land use planning.

6. Acknowledgement: The authors extend their gratitude Centre for Water and Geospatial Studies, Tamil Nadu Agricultural University and Division of Agricultural Physics, in preparing and successfully submitting this manuscript. furthermore, the authors express appreciation to their colleagues and the reviewers who offered constructive feedback and recommendations to enhance the quality of the manuscript

7. Funding: This research did not receive any funds

References:

Ahmed, R., Zafor, M. A., & Trachte, K. (2024). Land-use and land-cover changes in Cottbus city and Spree-Neisse district, Germany, in the last two decades: a study using remote sensing data and Google Earth Engine. Remote Sensing, 16(15), 2773. https://doi.org/10.3390/rs16152773

Aklilu Tesfaye, A., & Gessesse Awoke, B. (2021). Evaluation of the saturation property of vegetation indices derived from sentinel-2 in mixed crop-forest ecosystem. Spatial Information Research, 29(1), 109–121. https://doi.org/10.1007/s41324-020-00339-5

Aksoy, S., Yildirim, A., Gorji, T., Hamzehpour, N., Tanik, A., & Sertel, E. (2022). Assessing the performance of machine learning algorithms for soil salinity mapping in Google Earth Engine platform using Sentinel-2A and Landsat-8 OLI data. Advances in Space Research, 69(2), 1072–1086. https://doi.org/10.1016/j.asr.2021.10.024

Alexandridis, T. K., Ovakoglou, G., & Clevers, J. G. (2020). Relationship between MODIS EVI and LAI across time and space. Geocarto international, 35(13), 1385–1399. https://doi.org/10.1080/10106049.2019.1573928

Awad, M. (2021). Google Earth Engine (GEE) cloud computing-based crop classification using radar, optical images and Support Vector Machine Algorithm (SVM) (pp. 71–76). Presented at the 2021 IEEE 3rd International Multidisciplinary Conference on Engineering Technology (IMCET), IEEE. https://doi.org/10.1109/IMCET53404.2021.9665519

Bajocco, S., Ferrara, C., Savian, F., Ginaldi, F., Puletti, N., & Crecco, L. (2024). LAIr: an R package to estimate LAI from Normalized Difference Vegetation Index. SoftwareX, 27, 101776. https://doi.org/10.1016/j.softx.2024.101776

Bajocco, S., Ginaldi, F., Savian, F., Morelli, D., Scaglione, M., & Fanchini, D. (2022). On the use of NDVI to estimate LAI in field crops: Implementing a conversion equation library. Remote Sensing, 14(15), 3554. https://doi.org/10.3390/rs14153554

Belozerova, O. (2024). Enhancing WOFOST crop model with unscented Kalman filter assimilation of leaf area index. International Journal of Image and Data Fusion, 15(2), 174–189. https://doi.org/10.1080/19479832.2023.2287037

Bobée, C., Ottlé, C., Maignan, F., de Noblet-Ducoudré, N., Maugis, P., Lézine, A.-M., & Ndiaye, M. (2012). Analysis of vegetation seasonality in Sahelian environments using MODIS LAI, in association with land cover and rainfall. Journal of Arid Environments, 84, 38–50. https://doi.org/10.1016/j.jaridenv.2012.03.005

Boonma, R., Suwanprasit, C., & Homhuan, S. (2024). Modeling Rice Growth and Yield using Integrated Remote Sensing Data on Google Earth Engine. International Journal of Geoinformatics. https://doi.org/10.52939/ijg.v20i11.3693

Brinkhoff, J., McGavin, S. L., Dunn, T., & Dunn, B. W. (2024). Predicting rice phenology and optimal sowing dates in temperate regions using machine learning. Agronomy Journal, 116(3), 871–885. http://dx.doi.org/10.1002/agj2.21398

Cui, Y., Yang, G., Zhou, Y., Zhao, C., Pan, Y., Sun, Q., & Gu, X. (2023). AGTML: A novel approach to land cover classification by integrating automatic generation of training samples and machine learning algorithms on Google Earth Engine. Ecological Indicators, 154, 110904. https://doi.org/10.1016/j.ecolind.2023.110904

Delegido, J., Verrelst, J., Meza, C., Rivera, J., Alonso, L., & Moreno, J. (2013). A red-edge spectral index for remote sensing estimation of green LAI over agroecosystems. European Journal of Agronomy, 46, 42–52. https://doi.org/10.1016/j.eja.2012.12.001

Denis, A., Desclee, B., Migdall, S., Hansen, H., Bach, H., & Ott, P. (2020). Multispectral Remote Sensing as a Tool to Support Organic Crop Certification: Assessment of the Discrimination Level between Organic and Conventional Maize. Remote Sensing, 13(1), 117. https://doi.org/10.3390/rs13010117

Dong, T., Liu, J., Qian, B., Jing, Q., Croft, H., Chen, J., et al. (2016). Deriving maximum light use efficiency from crop growth model and satellite data to improve crop biomass estimation. IEEE Journal of Selected topics in Applied Earth observations and Remote sensing, 10(1), 104–117. https://doi.org/10.1109/JSTARS.2016.2605303

Drusch, M., Del Bello, U., Carlier, S., Colin, O., Fernandez, V., & Gascon, F.(2012). Sentinel-2: ESA's optical high-resolution mission for GMES operational services. Remote sensing of Environment, 120, 25–36. https://doi.org/10.1016/j.rse.2011.11.026

Ekwe, M. C., Adeluyi, O., Verrelst, J., Kross, A., & Odiji, C. A. (2024). Estimating rainfed groundnut's leaf area index using Sentinel-2 based on Machine Learning Regression Algorithms and Empirical Models. Precision Agriculture, 25(3), 1404–1428. https://doi.org/10.1007/s11119-024-10117-0

Gaikwad, S. V., Vibhute, A. D., & Kale, K. V. (2021). Estimation of area sown and sowing dates of in season *Rabi* crops using sentinel-2 time series data. The Journal of Research ANGRAU, 49(1), 69–81. https://epubs.icar.org.in/index.php/TJRA/article/view/133432

Ganjirad, M., & Bagheri, H. (2024). Google Earth Engine-based mapping of land use and land cover for weather forecast models using Landsat 8 imagery. Ecological Informatics, 80, 102498. https://doi.org/10.1016/j.ecoinf.2024.102498

Gautam, Y., & Singh, P. (2018). Economic analysis of sorghum in Maharashtra, India. International Journal of Agricultural and Statistical Sciences, 14(2), 601–606. https://www.phytojournal.com/archives/2021/vol10issue1S/PartB/S-10-1-20-375.pdf

Getahun, S., Kefale, H., & Gelaye, Y. (2024). Application of Precision Agriculture Technologies for Sustainable Crop Production and Environmental Sustainability: A Systematic Review. The Scientific World Journal, 2024(1), 2126734. https://doi.org/10.1155/2024/2126734

Gislason, P. O., Benediktsson, J. A., & Sveinsson, J. R. (2006). Random forests for land cover classification. Pattern recognition letters, 27(4), 294–300. https://doi.org/10.1016/j.patrec.2005.08.011

Gorelick, N., Hancher, M., Dixon, M., Ilyushchenko, S., Thau, D., & Moore, R. (2017). Google Earth Engine: Planetary-scale geospatial analysis for everyone. Remote sensing of Environment, 202, 18–27. https://doi.org/10.1016/j.rse.2017.06.031

Han, H., Liu, Z., Li, J., & Zeng, Z. (2024). Challenges in remote sensing based climate and crop monitoring: navigating the complexities using AI. Journal of cloud computing, 13(1), 34. https://doi.org/10.1186/s13677-023-00583-8

Hassanpour, R., Majnooni-Heris, A., Fakheri Fard, A., & Verrelst, J. (2024). Monitoring Biophysical Variables (FVC, LAI, LCab, and CWC) and Cropland Dynamics at Field Scale Using Sentinel-2 Time Series. Remote Sensing, 16(13), 2284. https://doi.org/10.3390/rs16132284

Immitzer, M., Vuolo, F., & Atzberger, C. (2016). First experience with Sentinel-2 data for crop and tree species classifications in central Europe. Remote sensing, 8(3), 166. https://doi.org/10.3390/rs8030166

Jiang, L., Huang, X., Wang, F., Liu, Y., & An, P. (2018). Method for evaluating ecological vulnerability under climate change based on remote sensing: A case study. Ecological indicators, 85, 479–486. http://dx.doi.org/10.1016/j.ecolind.2017.10.044

Jin, Z., Azzari, G., You, C., Di Tommaso, S., Aston, S., Burke, M., & Lobell, D. B. (2019). Smallholder maize area and yield mapping at national scales with Google Earth Engine. Remote sensing of environment, 228, 115–128. https://doi.org/10.1016/j.rse.2019.04.016

Jitendra, & Pant, T. (2024). Estimation of wheat crop production using multispectral information fusion. Journal of the Science of Food and Agriculture, 104(2), 1074–1084. https://doi.org/10.1002/jsfa.13030

Jones, M. O., Figueiredo, G., Howson, S., Toro, A., Rundquist, S., Garner, G., et al. (2024). Monitoring and Mapping a Decade of Regenerative Agricultural Practices Across the Contiguous United States. Land, 13(12), 2246. https://doi.org/10.3390/land13122246

Khan, M. S., Yadav, P., Semwal, M., Prasad, N., Verma, R. K., & Kumar, D. (2024). Predicting canopy chlorophyll concentration in citronella crop using machine learning algorithms and spectral vegetation indices derived from UAV multispectral imagery. Industrial Crops and Products, 219, 119147. https://doi.org/10.1016/j.indcrop.2024.119147

Klerkx, L., Jakku, E., & Labarthe, P. (2019). A review of social science on digital agriculture, smart farming and agriculture 4.0: New contributions and a future research agenda. NJAS-Wageningen journal of life sciences, 90, 100315. https://doi.org/10.1016/j.njas.2019.100315

Lillesand, T., Kiefer, R. W., & Chipman, J. (2015). Remote sensing and image interpretation. John Wiley& Sons. https://www.wiley.com/ensg/Remote+Sensing+and+Image+Interpretation%2C+7th+Edition-p-9781118343289

Maciel Junior, I. C., Dallacort, R., Boechat, C. L., Teodoro, P. E., Teodoro, L. P. R., Rossi, F. S., et al. (2024). Maize Crop Detection through Geo-Object-Oriented Analysis Using Orbital Multi-Sensors on the Google Earth Engine Platform. *AgriEngineering*, *6*(1), 491–508. https://doi.org/10.3390/agriengineering6010030

Mehedi, I. M., Hanif, M. S., Bilal, M., Vellingiri, M. T., & Palaniswamy, T. (2024). Remote Sensing and Decision Support System Applications in Precision Agriculture: Challenges and Possibilities. IEEE Access, 12, 44786–44798. https://doi.org/10.1109/ACCESS.2024.3380830

Meiyan, S., Qizhou, D., ShuaiPeng, F., Xiaohong, Y., Jinyu, Z., & Lei, M. (2022). Improved estimation of canopy water status in maize using UAV-based digital and hyperspectral images. Computers and electronics in agriculture, 197, 106982. https://dl.acm.org/doi/10.1016/j.compag.2024.108943

Mondschein, Z., Paliwal, A., Sida, T. S., Chamberlin, J., Wang, R., & Jain, M. (2024). Mapping Field-Level Maize Yields in Ethiopian Smallholder Systems Using Sentinel-2 Imagery. Remote Sensing, 16(18), 3451. https://doi.org/10.3390/rs16183451

Na, I. S., Lee, S., Alamri, A. M., & AlQahtani, S. A. (2024). Remote Sensing and AI-based Monitoring of Legume Crop Health and Growth. Legume research - an international journal. https://doi.org/10.18805/LRF-795

Pazhanivelan, S., Sudarmanian, N., Satheesh, S., & Ragunath, K. (2025). Innovative Approaches to Bengal gram Yield Mapping: Integration of Sentinel-1 SAR and Crop Simulation Models for Precision Agriculture. Journal of Scientific Research and Reports, 31(1), 449–460. https://doi.org/10.9734/jsrr/2025/v31i12788

Shaw, J., Ghosh, P., Bhattacharya, S., & Kundu, A. (2024). Combined drought and salinity trigger unique lncRNA regulatory signatures in sweet sorghum (Sorghum bicolor L. Moench) compared to individual stress responses. Plant Growth Regulation, 1–18. http://dx.doi.org/10.1007/s10725-024-01229-8

Shelestov, A., Lavreniuk, M., Kussul, N., Novikov, A., & Skakun, S. (2017). Large scale crop classification using Google earth engine platform (pp. 3696–3699). Presented at the 2017 IEEE international geoscience and remote sensing symposium (IGARSS), IEEE. https://doi.org/10.1109/IGARSS.2017.8127801

Singh, R., Singh, K., & Gohain, G. (2024). Simulating crop yield using the DSSAT v4. 7-CROPGRO-soyabean model with gridded weather and soil data. Modeling Earth Systems and Environment, 10(1), 845–853. http://dx.doi.org/10.1007/s40808-023-01807-1

Tenreiro, T. R., García-Vila, M., Gómez, J. A., Jiménez-Berni, J. A., & Fereres, E. (2021). Using NDVI for the assessment of canopy cover in agricultural crops within modelling research. Computers and Electronics in Agriculture, 182, 106038. https://doi.org/10.1016/j.compag.2021.106038

Turner, W., Rondinini, C., Pettorelli, N., Mora, B., Leidner, A. K., & Szantoi, Z.(2015). Free and open-access satellite data are key to biodiversity conservation. Biological Conservation, 182, 173–176. https://doi.org/10.1016/j.biocon.2014.11.048

Wang, H., & Zhao, H. (2020). Dynamic Changes of Soil Erosion in the Taohe River Basin Using the RUSLE Model and Google Earth Engine. Water, 12(5), 1293. https://doi.org/10.3390/w12051293

Wang, M., Huang, L., Tang, B.-H., Yu, Y., Zhang, Z., Wu, Q., & Cheng, J. (2024). Mapping cropland in Yunnan Province during 1990–2020 using multi-source remote sensing data with the Google Earth Engine Platform. Geocarto International, 39(1), 2392848. https://doi.org/10.1080/10106049.2024.2392848

Welles, J. M., & Norman, J. (1991). Instrument for indirect measurement of canopy architecture. Agronomy journal, 83(5), 818–825. https://doi.org/10.2134/agronj1991.00021962008300050009x

Wu, Q., Wang, X., Chen, S., Wang, L., & Jiang, J. (2023). Land Surface Greening and CO2 Fertilization More than Offset the Gross Carbon Sequestration Decline Caused by Land Cover Change and the Enhanced Vapour Pressure Deficit in Europe. Remote Sensing, 15(5), 1372. https://doi.org/10.3390/rs15051372

Yash Gautam, PK Singh and OP Singh. Financial profitability and resource use efficiency in sorghum production under rainfed condition. J Pharmacogn Phytochem 2021;10(1S):106-109. https://www.phytojournal.com/archives/2021/vol10issue1S/PartB/S-10-1-20-375.pdf

Yan, L., Roy, D. P., Zhang, H., Li, J., & Huang, H. (2016). An automated approach for sub-pixel registration of Landsat-8 Operational Land Imager (OLI) and Sentinel-2 Multi Spectral Instrument (MSI) imagery. Remote Sensing, 8(6), 520. https://doi.org/10.3390/rs8060520

Zhao, D., Huang, J., Li, Z., Yu, G., & Shen, H. (2024). Dynamic monitoring and analysis of chlorophyll-a concentrations in global lakes using Sentinel-2 images in Google Earth Engine. Science of The Total Environment, 912, 169152. https://doi.org/10.1016/j.scitotenv.2023.169152